21st Australasian Fluid Mechanics Conference
Adelaide, Australia
10-13 December 2018

Numerical Study of Interactive Flow Field for a Canard Rotor Wing Aircraft

W. Sun[1], H. Wang[1] and Z.-J. Shang[1]

[1]Department of Engineering Mechanics
Chang'an University, Xi'an, ShannXi Province 710064, China

Abstract

The interactive flow field of a Canard Rotor Wing(CRW) aircraft with two different tail arrangements, H-tail and T-tail, are investigated by numerically solving three dimensional steady fully turbulent Reynolds Averaged Navier-Stokes (RANS) equations. The rotor/wing is modelled using momentum sources method. The variations of normal force and longitudinal moment of the fuselage in hover and forward flight are analysed with the canard and horizontal tail deflection angle set at 0°, 10° and 20°, respectively. The result shows that, in hover, the tail arrangement has almost no impact on the aerodynamics of the aircraft, but in forward flight, the T-tail produces less normal force loss and less nose-up pitching moment, implying that the T-tail arrangement provides more advantages, and H-tail arrangement is considered inappropriate for the CRW aircraft.

Introduction

The value of high speed rotorcraft is undeniable, particularly for rescue missions and military warfare applications. Aircraft designers are constantly looking for ways to make them practicable, numerous high speed rotorcraft concepts have been developed. The CRW aircraft is the most promising one of these concepts[1]. Its key characteristic is a specially designed stoppable rotor/wing, which can circumrotate in high speed like a rotor as well as be locked and used as a fixed wing. That makes the aircraft have the abilities of taking off and landing vertically like a helicopter and cruising in a high speed like a fixed wing aircraft [2]. Besides, the CRW aircraft has a "canard" fore-plane as well as a conventional tail-plane, allowing both to contribute lift during forward flight and to offload the rotor/wing. It is a typical three-surface configuration after conversion. Figure 1 shows the normal configuration for a CRW aircraft.

Figure 1. Normal configuration of a CRW aircraft, X-50A

The history of the stoppable rotor concept can be traced back to early 1930s, Herrick flew a biplane, the HV-1, which was equipped with a top wing that could be unlocked in flight to permit autorotation. The upper wing airfoil section was symmetrical to allow it work in both modes. From then on, such stoppable rotor/wing attracted widespread attention and had been further developed. The so called CRW concept was first proposed in 1990 by McDonnal Douglas Helicopter Company (now the Boeing company) [3]. During 1990-2005, the CRW concept has been thoroughly studied by Boeing Corporation, and a famous demonstrator known as "Dragonfly" X-50A [4] has been produced. Unfortunately, the prototype aircraft never successfully transitioned to full forward flight due to inherent design flaws. The vehicle crashed, subsequent investigation revealed that the aircraft's fuselage was subject to an aerodynamic pitching moment of extreme sensitivity [5]. It may be related to the downwash flow. In recent years, the investigations have been made to explore the potential application by Korea [6], and some Chinese scholars have been working on the key technology breakthrough [7][8][9].

Obviously, it is the strong interaction between rotor/wing and the aerodynamic surfaces that makes the aircraft unstable and out of control. Throughout the history of the CRW's development, the H-tail arrangement is always used because the H-tail provides a lot of advantages. It can position the vertical tails out of the rotor wash and can serve to hide the hot engine nozzle from heat-seeking missiles when viewed from an angle off the rear of the aircraft. However, the position of the horizontal tail maybe too low to avoid the rotor wash, and it may be the real root cause of the X-50A's crashes. In order to study the effect of horizontal tail height, the H-tail and T-tail arrangements are investigated. Since the quantity of interaction is what we need, rather than the unsteady instantaneous aerodynamics of the flow field, the momentum source method [10] is used in the present paper. The rotor wing is modeled as a distribution of momentum sources. In order to increase the accuracy, an airfoil coefficient table is used to compute the blade element forces, and the Prandtl's Tip Loss Function [11] is used to describe the blade tip loss.

Computational Method

Due to the rotor modeling technique in the momentum source method, only steady–state solutions are desired. The three-dimensional compressible steady RANS equations are chosen as the governing equations. The non-dimensional form of the governing equations in Cartesian coordinates can be written as follows:

$$\frac{\partial Q}{\partial t}+\frac{\partial (E-E_v)}{\partial x}+\frac{\partial (F-F_v)}{\partial y}+\frac{\partial (G-G_v)}{\partial z}=F_{source} \quad (1)$$

The flow solver used in this paper is an in-house multi-block RANS solver. In this code, temporal marching method is implicit Lower-upper Symmetric-Gauss-Seidel (LU-SGS) [13]. The spatial discretization scheme for convection terms is Roe scheme [14] with Harten's entropy correction. 3rd-order Monotonic Upstream-Centered Scheme for Conservation Laws (MUSCL) reconstruction method is used to increase the Roe scheme to 2nd-order. The viscous fluxes are discretized with 2nd-order centered schemes. In order to overcome the difficulty in solving compressible equations for low-Ma flows, Weiss and Smith preconditioning matrix [15] is introduced. The no-slip wall boundary condition is applied for the viscous wall. The far field boundary condition is typically based on Riemann invariants.

For turbulence model equations, implicit LU-SGS method is also operated as time marching scheme, which is similar to the discretization of governing equations. Convection terms therein

are discretized by 1st-order upwind schemes, while production terms and destruction terms are treated explicitly and implicitly respectively to increase the numerical robustness.

The term F_{source} to take special note of on the right hand side of the above equations is the source term vector, which is introduced to model the rotor/wing. Precise modelling of a helicopter rotor is a difficult challenge. The rotational motion of the blades with respect to the fuselage ensures that the aerodynamic problem is naturally unsteady. The complexity is further compounded by the strong mutual interference effects of the blades and the aerodynamic surfaces. The momentum source method was originally proposed by Rajagopalan and Fanucci for the analysis of vertical axis wind turbines and later extended to helicopter rotors [16]. The rotor is modeled as a set of forces that are applied to the flow field in cells intersecting the rotor disk. Firstly, the rotor wing is discretized into spanwise elements by circles drawn from the rotor center. Then compute the lift and drag forces on the elements using Blade Element Theory. An airfoil coefficient table is used here to compute the lift and drag more exactly. The lift and drag coefficients of the airfoil are all from wind tunnel [17][18], and blockage correction and scale effects have been considered. The force vector $(f_x, f_y, f_z)^T$ acting on the blade element can be obtained after projection in the coordinates, $(-f_x, -f_y, -f_z)^T$ is then the instantaneous force acting on the fluid element according to Newton's Third Law. But the truth is that the force exists only when the rotor/wing is passing through this control volume, the source terms must be time averaged before added to the control equations. The time averaged source term vector can be written as

$$F_{source} = \frac{N_b \Delta\phi}{2\pi}\left(-f_x, -f_y, -f_z\right)^T \qquad (2)$$

Where N_b is the number of blades, $\Delta\phi$ is the angular distance through which the blade rotates in passing through the control volume.

Model and Mesh

The CRW aircraft consists of rotor wing, canard, horizontal tail, vertical tail and fuselage. A summary of the main parameters of model are shown in table 1. The planform of rotor blades is isosceles trapezoid. The rotor blades are untwisted and are comprised of elliptic airfoil section with 16% thickness. The canard and horizontal tail are all moveable.

Name of parameter	Symbol	Value
Radius of rotor wing	R	0.978m
Airfoil chord	C_{tip}	0.17m
Taper ratio	λ	2
Fuselage Length	L_f	3m

Table 1. Main parameters of CRW

The landing gear and the rotor hub are ignored for simplifying. The CFD model of the CRW configuration with an actuator disk and the computational grids are shown in figure 2. The grid on the disk plane is of (61×417×1) nodes that is 61 nodes are along the radial, 417 nodes are along the circumference. The far field boundary is formed by a cuboid. It's 20 times of the length of fuselage far away from the rotor center. The origin of the coordinates is located at the center of the rotor. Multiblock structured grid is used to discretize the computational domain. The total number of grid cell is 1.3×10^7 for H-tail case, and $1.4\times10^7$for T-tail case. Using these grids the flow fields for CRW aircraft in hover and forward flight are simulated.

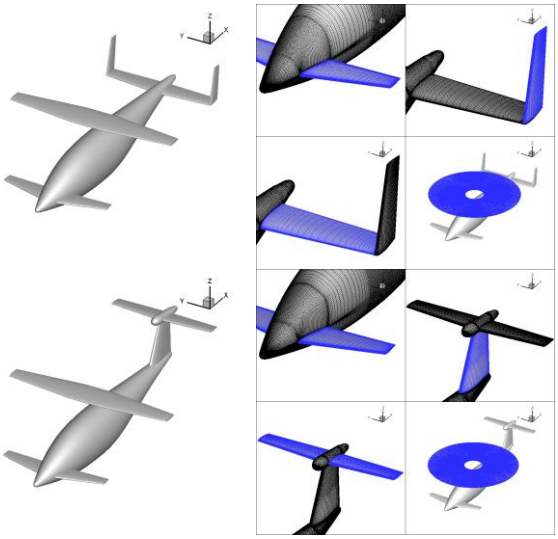

Figure 2. CFD model of the CRW configuration with an actuator disk and grid

Results and Discussions

Due to the hover and low speed forward flight are the most important flight status when the CRW aircraft flies in rotary-wing mode, the hover and two advance ratios, that are μ=0.06 and μ=0.12, have been chosen for numerical simulation in this study. The corresponding free stream velocity are 0m/s, 5m/s and 10m/s, respectively. The rotor/wing collective angle is set at 10 °for all cases, and the deflection angle of the canard and horizontal tail are set at 0 °, 10 °and 20 °, respectively.

In figure 3, the thrust coefficient C_T at different collective angles for the two tail arrangements are plotted in comparison with the experimental data obtained on the ground. It is clear to see that experimental C_T increases as the collective angle increases, and at the same collective angle, the C_T of T-tail arrangement is a little larger than that of H-tail arrangement but not by much. In general, the numerical results are in good agreement with the experimental data, the trends are well predicted, which validates the present numerical method. However, there are two points that need attention, first, the deviation shows up between computation result and experimental data at low collective angles (θ= 0° and θ= 2°), which implies that an important aspect of the experimental geometry has not been adequately modeled in the computational technique or that there is error in the experimental value, obviously, the later one is reasonable; second, the computational result shows little difference between two tail arrangements, indicating tail arrangement has almost no impact on the rotor/wing's performance in hover.

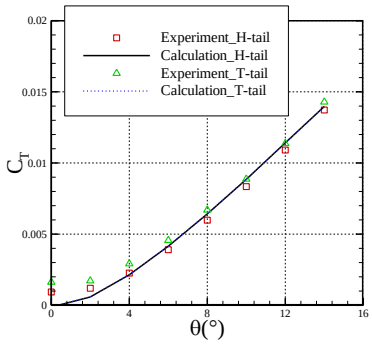

Figure 3. Thrust in hover

Figure 4 and figure 5 show the variation of fuselage normal force with canard/horizontal tail deflection angle for H-tail and

T-tail arrangement. The normal force is positive up, and the force coefficient is defined as $C_z = F_z/\frac{1}{2}\rho(\Omega R)^2 \pi R^2$, where ρ is the air density and a constant value of 1.225kg/m^3 was used here, Ω is the rotational speed. The computational results show similar trends for both tail arrangements. For hover flight, as the deflection angle of canard increases, the normal force loss decreases, and as the deflection angle of the horizontal tail increases, the normal force stays almost constant, indicating the canard is within the rotorwash and plays a more important role in reducing the normal force loss in hover. Hence, the canard deflection angle should be as large as possible to reduce the block of flow through the rotor disk when fly vertically or in hover. For forward flight, as the canard/horizontal angle increases, the normal force loss decreases, and this trend becomes apparent as the forward speed increases. Especially when the advance ratio μ increases to 0.12, both the canard deflection and horizontal tail deflection have great impact on the normal force loss. It is not difficult to understand that when the deflection angle is zero, the downwash is the dominant characteristic and the aerodynamic surfaces produce no lift, leading to relative large normal force loss; as the deflection angles increase, both canard and horizontal tail produce lift, the normal force loss decreases. Comparison of the normal force loss between H-tail and T-tail arrangement shows a very interesting point to note, the normal force loss of T-tail arrangement is greatly reduced compared with the H-tail arrangement during forward flight, indicating the T-tail arrangement lifts the horizontal tail clear of rotorwash.

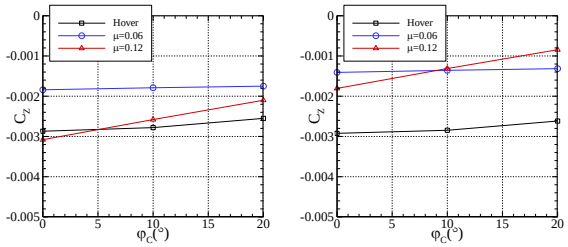

(a)H-tail (b)T-tail

Figure 4. Variation of fuselage normal force with canard deflection angle

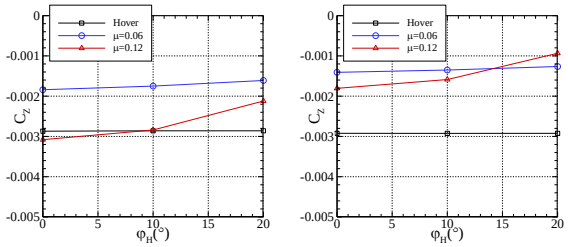

(a)H-tail (b)T-tail

Figure 5. Variation of fuselage normal force with horizontal tail deflection angle

Figure 6 and figure 7 show the variation of fuselage pitching moment with canard/horizontal tail deflection angle for H-tail and T-tail arrangement. The pitching moment is defined as positive nose-up, and $C_{my} = M_y/\frac{1}{2}\rho(\Omega R)^2 \pi R^2 R$. The centre of moment is the centre of gravity, which is located at 0.585m below the centre of the rotor wing. The general trends of the pitching moment are similar for both H-tail and T-tail arrangement. For hover flight, the canard is within rotor wash and produces strong nose down moment because of the negative normal force. Hence, as the canard deflection angle increases, the nose-down pitching moment decreases slightly. The horizontal tail is not influenced by the rotor wash, so that the pitching moment stays almost constant as the deflection angle of the horizontal tail increases. For forward flight, the pitching moments become positive. The sudden change of pitching moment (from nose-down moment to nose-up moment) at any time is not good for aircraft's control. It can cause fatal accident if this nose-up pitching moment is too large or too abrupt. As the deflection angle of canard increases, the nose-up pitching moment increases, and as the deflection angle of the horizontal tail increases, the nose-up pitching moment decreases, implying that the horizontal tail is the key aerodynamic surface to trim a CRW aircraft. For T-tail arrangement at μ=0.12, the pitching moment decreases to zero at about φ_H=15°, as illustrated in figure 7. Comparison of the pitching moment between H-tail and T-tail arrangement shows another advantage of T-tail arrangement, because the T-tail arrangement lifts the horizontal tail clear of rotorwash during forward flight, the nose-up pitching moment is much smaller, making the vehicle easier to trim.

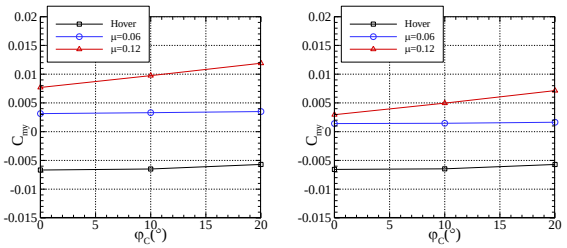

(a)H-tail (b)T-tail

Figure 6. Variation of fuselage pitching moment with canard deflection angle

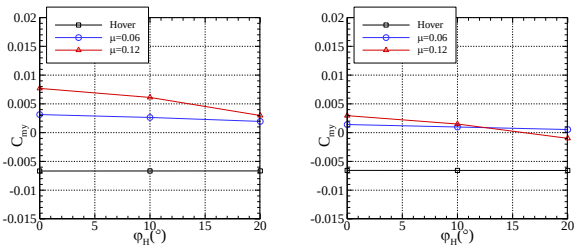

(a)H-tail (b)T-tail

Figure 7. Variation of fuselage pitching moment with horizontal tail deflection angle

The characteristics of aerodynamic force and moment of the CRW aircraft are ultimately determined by the rotor/wing's downwash flow. The streamlines for CRW aircraft with H-tail and T-tail in different flight status predicted by the present method are plotted in figure 8. For hover flight, the rotor/wing's influence can be seen clearly by the wake flow contraction when passing through the disk. For forward flight, the airflow flows downward and backward after passes through the rotor disk. As the speed of forward flight increases, the rotor downwash shifts backward apparently. The flow fields around the front half of the fuselage for H-tail and T-tail arrangement are much the same. However, the flow fields around the horizontal tails are significantly different from each other. The T-tail arrangement lifts the horizontal tail, makes it out of the rotor wash all the time.

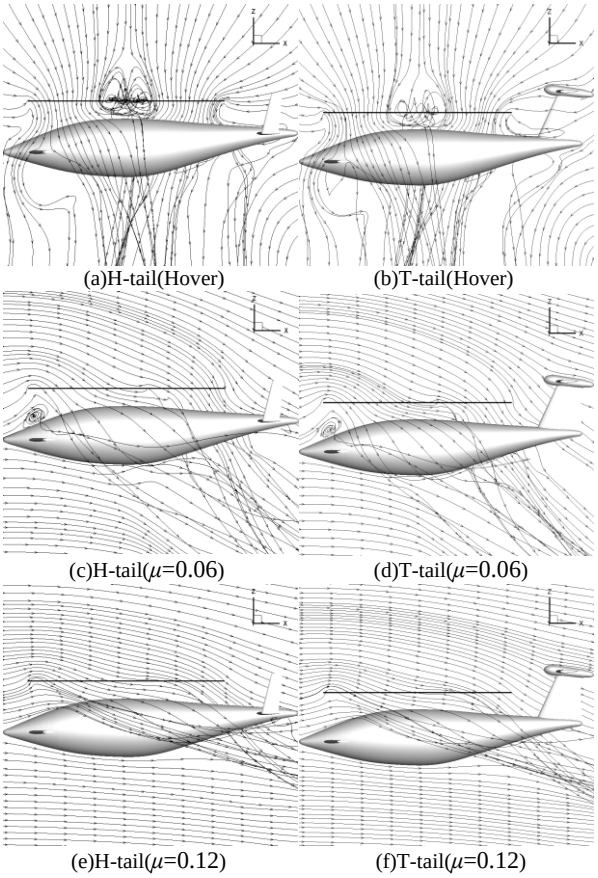

Figure 8. Streamlines comparison for CRW with H-tail and T-tail in different flight status

Conclusions

The three-dimensional steady fully turbulent RANS equations with momentum source terms have been used to simulate the interactive flow fields of the Canard Rotor Wing aircraft with different tail arrangements in hover and forward flight. The momentum source method is improved by using an airfoil coefficient table to compute the blade element forces and Prandtl's tip loss function to take the blade tip loss into account.

For hover flight, the computational rotor thrust is in agreement with experimental data, the tail arrangements has little influence on the performance of the rotor/wing; the higher deflection angle of canard, the less normal force loss and nose-down pitching moment, implying the canard is required to deflect with as large angle as possible; The deflection angle of Horizontal tail has little influence on the aircraft's normal force and pitching moment, implying the rotorwash is avoided by both H-tail and T-tail.

For forward flight, the general trends of the normal force and pitching moment are similar for H-tail and T-tail arrangement. Because both canard and horizontal tail are important lifting surfaces in forward flight, the higher deflection angle of canard/horizontal tail, the less normal force loss. The variation of pitching moments with the horizontal tail's deflection reflects the important role of the tail arrangement. T-tail arrangement produces less normal force and nose-up pitching moment compared with H-tail arrangement, implying the rotorwash shifts backward and affects the performance of the tail plane. Compare with the H-tail arrangement, the T-tail arrangement would be a more appropriate choice for CRW aircraft.

References

[1] Clark A. Mitchell, Barbara J. Vogel. The Canard Rotor Wing (CRW) aircraft- a new way to fly. AIAA 2003-2517

[2] Deng Yang-ping, Gao Zheng-hong, Zhan Hao. Development and Key Technologies of CRW. Flight Dynamics 2006; 24(3):1~4 (in Chinese)

[3] Rutherford, J. Technology needs for high-speed rotorcraft. NASA CR-177578

[4] X-50 Dragonfly Canard Rotor/Wing (CRW). Global Security.org. Retrieved 2009-03-13.

[5] McKenna, James T. One step beyond. Rotor & Wing, February, 2007, P: 54.

[6] C. Kim, J. Lee. Hub drag reduction strategies of Canard Rotor/Wing unmanned vehicles. Journal of aircraft 2007; 44(4): 1388-1390.

[7] Deng Yangping, Gao Zhenghong, Zhan Hao. Experimental investigation on aerodynamic interactions of canard rotor/wing aircraft in hover and low speed forward flight. Journal of Experimental Mechanics 2009; 24(6):563-567.

[8] Sun Wei, Gao Zhenghong, et al. Aerodynamic characteristics of hovering rotor/wing. Acta Aerodynamica Sinica 2015; 33(2):232-238.

[9] Li Yibo, Ma Dongli. Numerical simulation of rotor-aerodynamic surface interaction in hover using moving chimera grid. Chinese Journal of Aeronautics 2012; 25(3):342-348.

[10] Rajagopalan, R. G. and Fanucci, J. B. Finite Difference Model for vertical Axis Wind turbines. Journal of propulsion and power 1985; 1(6): 432-436.

[11] J. Gordon Leishman. Principles of helicopter aerodynamics. Cambridge University Press.

[12] Spalart PR, Allmaras SR. A one–equation turbulence model for aerodynamic flows. 30th Aerospace Sciences Meeting & Exhibit; 1992 January 6-9; Reno, NV. AIAA Paper No.: 92-0439.

[13] Yoon, S, Jameson, A. Lower-Upper Symmetric-Gauss-Seidel Method for the Euler and Navier-Stokes Equations. AIAA Journal 1988;26(9):1025-1026.

[14] Roe PL. Approximate Riemann Solvers, Parameter Vectors, and Difference Schemes. Journal of Computational Physics 1981;43: 357-372.

[15] Weiss JM, Smith WA. Preconditioning Applied To Variable and Constant Density Flow. AIAA Journal 1995;33(11):2050-2057.

[16] David M. O'Brien. Analysis of computational modeling techniques for complete rotorcraft configurations. Ph.D dissertation. Georgia Institute of Technology, May, 2006.

[17] Zhan H, Deng YP, Gao ZH. Investigation on aerodynamics performance of elliptic Airfoil at Low Speed. Aeronautical Computing Technique 2008;38(3):25-27 [Chinese]

[18] Deng YP, Gao ZH, Zhan H, Huang JT. Investigation on aerodynamics performance of elliptic airfoil at high speed. Aeronautical Computing Technique 2009;39(6):18-20 [Chinese]